

# NONLINEAR LATTICE OPTIMIZATION FOR THE SPring-8 UPGRADE

K. Soutome<sup>\*1,2</sup>, Y. Shimosaki<sup>1</sup>, M. Takao<sup>1</sup>, H. Tanaka<sup>2</sup>

<sup>1</sup>JASRI, Hyogo 679-5198, Japan

<sup>2</sup>RIKEN SPring-8 Center, Hyogo 679-5148, Japan

## Abstract

The SPring-8 upgrade project has adopted the hybrid MBA lattice to achieve the emittance of about 100 pmrad at 6 GeV. This optics has two dispersion bumps in a unit cell where chromaticity-correcting sextupoles locate. The horizontal and vertical betatron phases between these bumps are tuned to be about  $3\pi$  and  $\pi$ , respectively, to cancel the low order contributions of nonlinear kicks due to sextupoles. However, it is not easy to obtain a sufficiently large dynamic aperture (DA) since (i) the cancellation is incomplete due to a nested arrangement, (ii) sextupoles are very strong, and (iii) the number of tuning knobs is limited. The DA is quite small due to the leakage of nonlinear kicks by nested sextupoles. We hence proposed to install additional weak sextupoles between the dispersion bumps to suppress the leakage kick further. Simulations show that this simple scheme is very effective for suppressing amplitude-dependent tune shift (ADTS) and for enlarging DA.

## INTRODUCTION

The SPring-8 upgrade project is ongoing, aiming at an extremely small electron beam emittance for generating highly brilliant and highly coherent X-rays [1, 2]. To this end, we adopted a 5-bend achromat lattice as shown in Fig. 1 for the new storage ring (SPring-8-II). Machine parameters of the new ring are listed in Table 1. The natural emittance is 157 pmrad at 6 GeV and it is expected to be reduced to about 100 pmrad with the use of the radiation damping effect by insertion devices.

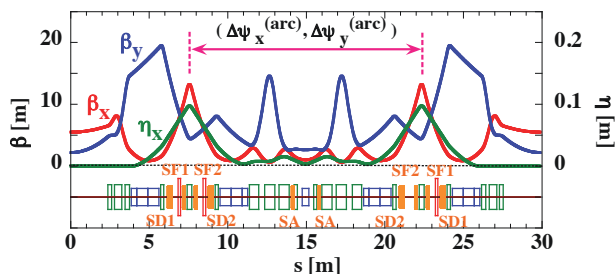


Figure 1: A unit cell of the 5-bend achromat lattice. The betatron functions  $\beta_x$  and  $\beta_y$  and the dispersion function  $\eta_x$  are shown. The arrangement of bending, quadrupole, sextupole and octupole magnets is shown by the blue, green, orange (solid) and red boxes, respectively.

As seen from Fig. 1, there are two "dispersion bumps" in a cell and strong sextupole magnets, indicated as SF and SD,

\* soutome@spring8.or.jp

Table 1: Machine Parameters of the Present and New Ring

	New Ring	Present Ring	
Lattice Type	5BA	DB	
Energy [GeV]	6	8	
Circ. [m]	1435.45	1435.95	
Nat. Emittance	0.157	6.6	A <sup>#1</sup>
[nmrad]		2.4	NA <sup>#2</sup>
Tune ( $\nu_x, \nu_y$ )	(108.10, 44.58)	(40.15, 18.35) A	(41.14, 19.35) NA
Nat. Chrom.	(-143, -147)	(-90, -41)	A
( $\xi_x, \xi_y$ )		(-117, -47)	NA
Beta at Straight	(5.5, 2.2)	(24.4, 5.8)	A
( $\beta_x, \beta_y$ )		(31.2, 5.0)	NA
Mom. Compct.	3.24e-5	1.46e-4	A
		1.60e-4	NA
Ene. Spread [%]	0.093	0.109	

<sup>#1</sup>A: Achromat Optics, <sup>#2</sup>NA: Non-Achromat Optics

are placed inside these arcs for correcting natural chromaticities. The betatron phase difference between the two arcs  $\Delta\psi^{(arc)}$  is basically set to  $(2n+1)\pi$  to cancel dominant effects of non-linear kicks due to these sextupoles. Though the phase matching between arcs (interleaved-sextupole scheme [3–5]) works to a certain extent, the cancellation is not perfect and it is not easy to obtain a sufficiently large dynamic aperture (DA). This is mainly due to a nested arrangement of strong sextupoles and DA is affected by the leakage of nonlinear kicks. In optimization procedures we tried to suppress this effect by detuning the betatron phase difference between the arcs [6] and optimizing the working point. Since the number of tuning knobs is limited and chromaticity-correcting sextupoles are strong, being about six times stronger than that for the present double-bend lattice, the degree of leakage suppression is not enough for widening DA so as to assure the stable beam operation.

In order to break this limitation, we thought up a new correction scheme of lattice nonlinearity that we introduce an auxiliary weak sextupole in the middle of a unit cell and adjust its strength to further cancel the leakage kicks. If this correction scheme works, leakage kicks from a unit cell will be reduced and this will widen DA. We first checked the effectiveness of this scheme by using a simple model and found that it indeed works. We then applied it to the SPring-8-II lattice and obtained a much larger DA than before. In Fig. 1 the sextupole indicated as SA is the auxiliary one. The integrated strength of SA is about 1/12 of the strongest sextupole SD1.

We also point out the importance of higher order effects. For a ring with very strong sextupole magnets, the higher-order terms in sextupole strength govern the behavior of electrons at large oscillation amplitudes. The well-known lowest-order ADTS formulae are no longer effective for describing tune variations at large amplitudes near a border of DA because of the dominant contributions from the higher-order terms. We hence developed a fourth-order formula of ADTS for describing tune variations at large horizontal amplitudes [7]. The formulae can predict tune variations near a border of DA and are useful for evaluating the contribution of higher order terms. In what follows we present details of our correction scheme of using weak sextupoles and show that the contribution of higher order terms is well suppressed.

## SUPPRESSION OF LEAKAGE KICKS BY WEAK SEXTUPOLES

As explained in the Introduction, we propose to install an auxiliary weak sextupole in the middle of a unit cell for suppressing lattice nonlinearity caused by the leakage of non-linear kicks by strong sextupoles. To check the effectiveness of this scheme, we first apply it to a toy model.

### Calculations with Toy Model

The purpose of this section is to check whether or not the weak sextupole SA can control the higher order terms by leakage kicks due to chromaticity-correcting sextupoles. For this purpose, we use a simple model as shown in Fig. 2 to extract the nature of a cancellation mechanism. In this model we assume the following: (i) Two families of sextupoles SF and SD are used for chromaticity correction to simplify the nested structure. (ii) Linear optics parameters at sextupoles are not essential for the present purpose and we assume that  $\beta_x=5\text{m}$  and  $\alpha_x=0$  at all sextupole positions and the tune difference is set to detuned values of  $\nu_A=0.025$  and  $\nu_B=0.67$ , which represent an example case of the SPring-8-II lattice. (iii) The vertical oscillation amplitude is small and we perform one-dimensional calculations in the horizontal direction.

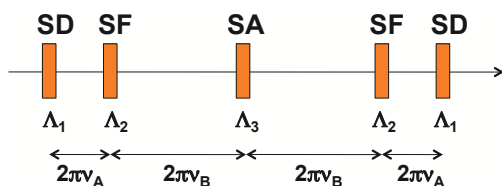


Figure 2: A toy model for checking the weak-sextupole correction scheme. The  $\Lambda_i = B''L/(B\rho)/2$  is the sextupole strength.

To determine the strength of sextupoles  $\Lambda_i$  we require that the lowest order coefficient of ADTS vanishes ( $\partial\nu_x/\partial J_x=0$ ) and the local horizontal chromaticity in the arc is fixed under the assumption that the dispersion function takes the same value at SF and SD ( $\Lambda_1 + \Lambda_2 = \text{const.}$ ).

With these constraints the strength of SF ( $\Lambda_1$ ) and SD ( $\Lambda_2$ ) are uniquely determined, once the strength of SA ( $\Lambda_3$ ) is given. Figure 3 shows the strength of sextupoles thus determined. By using this mode, we made tracking calculations to obtain ADTS and the Poincaré map in the horizontal direction. Results are shown in Fig. 4 for typical three cases of  $\Lambda_3=0, \pm 4\text{ m}^{-2}$ .

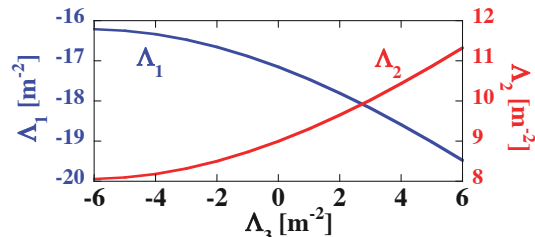


Figure 3: The sextupole strength  $\Lambda_1$  and  $\Lambda_2$  determined for a given value of  $\Lambda_3$ .

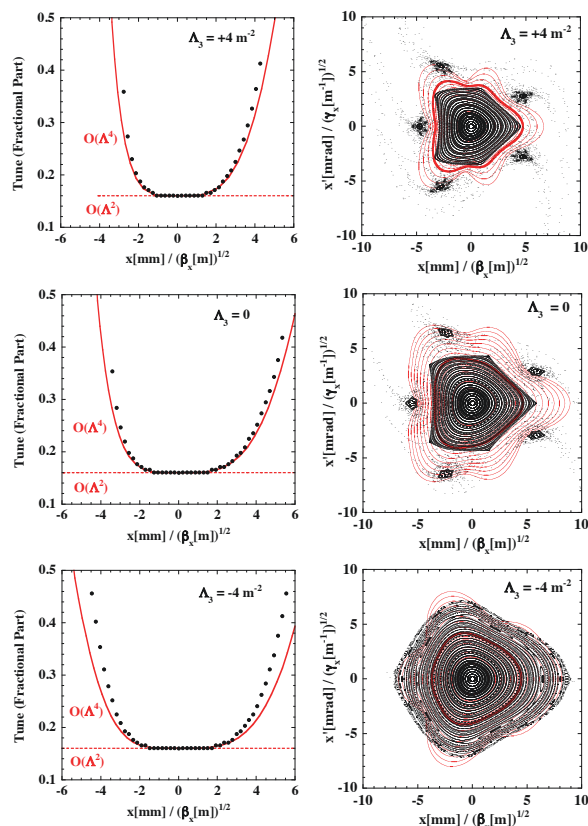


Figure 4: ADTS (left) and the Poincaré map (right) calculated for a toy model. Markers represent tracking simulation results and red solid curves are analytic calculations by using perturbation formulae. In the ADTS figures (left) dashed curves are for the lowest order perturbation and solid curves are for the fourth order perturbation. The bold red curve in the Poincaré map (right) is just for guiding eyes, which corresponds to the action of  $J_x = 8 \times 10^{-6}$  m.

To analyze the tracking simulation results we also applied higher-order ADTS formulae that we have developed up to

fourth order in sextupole strength [7]. These formulae have been derived by using the canonical perturbation theory [8] and are written in the following form:

$$v_x = v_{x0} + 2c_{xx}J_x + c_{xy}J_y + 3c_{xxx}J_x^2 + 2c_{xxy}J_xJ_y$$

$$v_y = v_{y0} + c_{xy}J_x + 2c_{yy}J_y + c_{xyy}J_x^2$$

These are valid when the amplitude of vertical betatron oscillation is smaller compared with the horizontal one. The coefficients on the right-hand side can be calculated in an analytic way by carrying out numerical integrals. The results are shown by red solid curves in Fig. 4. The ADTS is shown on the left side and we can clearly see that the suppression of only the lowest order terms (dashed curves) is insufficient and higher order contributions (solid curves) dominate the beam behavior near a border of stable region. We also see that at  $\Lambda_3 = -4 \text{ m}^{-2}$  the ADTS is flatter than at  $\Lambda_3=0$ , which means that higher order terms have been suppressed by introducing the weak sextupole SA. This is also seen from the Poincaré map shown on the right side.

### Application to SPring-8-II Lattice

We applied the above scheme to the SPring-8-II lattice and introduced weak sextupoles which are indicated as SA in Fig. 1. After optimizing the strength of SA we obtained ADTS as shown in Fig. 5 by the red curve. For comparison, we also show ADTS without SA by the black dashed curve and that after correcting only by octupoles by the blue curve. In calculating the red curve all octupoles were turned off and only SA was used. From this figure we see that the range of flatness of ADTS for the case of using SA is wider than using octupoles. This means that when SA is used instead of octupoles, the contribution of fourth order terms becomes smaller and the source of lattice nonlinearity due to leakage kicks is better suppressed. Figure 6 shows the on-momentum DA calculated at an injection point. A high-quality beam will be injected from the XFEL linac (SACLA) [2] at  $x=-2 \text{ mm}$  and we see that the obtained DA is wide enough for accepting the injection beams.

For beam injection we modified the structure of two unit cells located upstream and downstream of the injection point to realize a high horizontal beta. In the previous lattice design [6] where auxiliary weak sextupoles SA were not used, the beta value took 30m and the modification of injection two cells broke the symmetry of the ring. The introduction of SA has now enlarged DA and relaxed the requirement of a beta value at an injection point from 30m to about 20m. Owing to this, the modification of injection cells could be done locally within a limited range and the betatron phase advance over an injection cell is kept unchanged (same as the normal cell). The betatron functions and phase at sextupole positions are also unchanged and the symmetry of the ring and hence the beam stability has been improved very much.

### SUMMARY

In this paper we presented a new scheme of using auxiliary weak sextupoles for suppressing lattice nonlinearity in

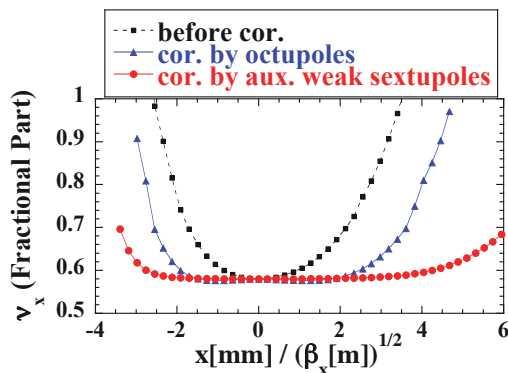


Figure 5: Calculated ADTS for the SPring-8-II storage ring.

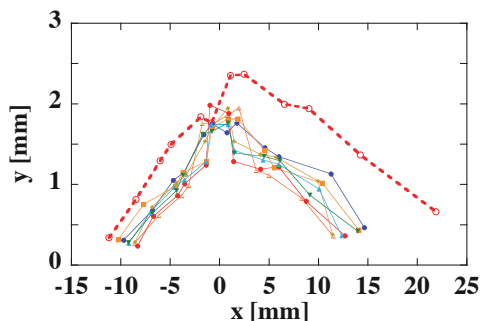


Figure 6: Dynamic aperture of on-momentum electrons for the SPring-8-II storage ring calculated at an injection point where  $\beta_x=20.1 \text{ m}$  and  $\beta_y=1.9 \text{ m}$ . The dashed curve is for the ideal ring without errors and solid curves are for the ring with sextupole misalignment in the range of  $\pm 50 \mu\text{m}$ .

the so-called hybrid MBA lattice [9, 10]. With the use of this scheme, ADTS could be made flatter and a wider DA was obtained. We also pointed out the importance of higher order contributions in discussing the behavior of electrons at large horizontal amplitudes. The betatron tune near a border of DA can be described well by the fourth order perturbation formulae that we developed. Our next target is to enlarge the momentum acceptance from the present value of 2% to 3% and nonlinear optimization studies are ongoing for this.

### REFERENCES

- [1] “SPring-8-II conceptual design report”, <http://rsc.riken.jp/pdf/SPring-8-II.pdf>, 2014.
- [2] H. Tanaka et al., “SPring-8 upgrade project”, in Proc. of IPAC’16, paper WEPOW019, p. 2867.
- [3] K. L. Brown, “A second-order magnetic optical achromat”, IEEE Trans. Nucl. Sci., vol. NS-26, p. 3490, 1979.
- [4] L. Emery, “An ultra-low emittance damping ring lattice and its dynamic aperture”, in Proc. of PAC’89, p. 1225.
- [5] K. Oide and H. Koiso, “Dynamic aperture of electron storage rings with noninterleaved sextupoles”, Phys. Rev., vol. E47, p. 2010, 1993.
- [6] K. Soutome et al., “Non-linear optimization of storage ring lattice for the SPring-8 upgrade”, in Proc. of IPAC’16, paper THPMR022, p. 3440.

- [7] K. Soutome and H. Tanaka, in preparation for publication.
- [8] R. D. Ruth, “Single-particle dynamics in circular accelerators”, AIP Conf. Proc. 153, p. 150, 1987.
- [9] L. Farvacque et al., “ESRF upgrade phase II status”, in Proc. of IPAC’14, paper MOPRO055, p. 79.
- [10] J-L. Revol et al., “ESRF upgrade phase II”, in Proc. of IPAC’13, paper TUOAB203, p. 1140.